Methods

Antibodies

Rabbit polyclonal antibody against mouse filamin A (FlnA) was raised by immunizing rabbits with a recombinant, dimerized domain of mouse FlnA.[1] Rabbit polyclonal antibody against human αIIb (SEW8) was raised by immunizing rabbits with purified human αIIb, which cross-reacts with murine αIIb. Mouse monoclonal antibody against Septin5 (LJ-33) was kindly provided by Dr. Jerry Ware (University of Arkansas). All other antibodies were commercially purchased and indicated in each section.

Immunoblotting

Platelets were isolated as described previously.[2] Washed platelets were resuspended in modified Tyrode-HEPES (Tyrode–N-2-hydroxyethylpiperazine-N-2-ethanesulfonic acid) buffer (10mM HEPES [pH 7.4], 12mM NaHCO3, 137mM NaCl, 2.7mM KCl, 5mM glucose, 0.25% bovine serum albumin [BSA]), and then lysed with equal volumes of T-SDS buffer (50 mM Tris-Cl [pH 7.4], 2% SDS) in the presence or absence of β-mercaptoethanol. Platelet lysates or cell lysates were analyzed by electrophoresis in 7.5% or 4-20% SDS-polyacrylamide gels. The separated proteins were then electrophoretically transferred to polyvinylidene fluoride (PVDF) membranes (Millipore), blocked with T-SDS containing 5% BSA, and then, probed with the antibodies described above. Blots were washed three times, incubated with a horseradish peroxidase (HRP)-conjugated secondary antibody, washed again three times, developed with Super Signal® West Pico Chemiluminescent Substrate (Thermo Scientific, Cleveland, OH), and analyzed using a ImageQuant LAS 4000 (GE Healthcare Biosciences, Piscataway, NJ).

Flow cytometric analysis

Platelets in whole blood were stained with PE-anti-mouse integrin αIIb (CD41) monoclonal antibody (mAb) (MWreg30: Santa Cruz Biotechnology Inc, CA, USA) and then incubated with 50 μg/ml of filipin (Sigma, St Louis, MO, USA) followed by flow cytometric analysis as previously described.[3] For microparticle analysis, whole blood samples were stained with PE-anti-mouse integrin αIIb mAb, and FITC-Annexin V (BD Biosciences, San Jose, CA, USA). Integrin αIIb-positive population was gated and further analyzed by FITC and forward-side scatter to discriminate Annexin V-positive platelets and platelet microparticles. Where indicated, blood samples were incubated with the mAbs that bind to GPVI (JAQ1; Emfret Analytics, Eibelstadt, Germany), integrin β1 (MB1.2; Millipore, Billerica, MA, USA), and CD31 (MEC 13.3; BD Pharmingen, San Diego, CA, USA) then, fixed with paraformaldehyde. After washing, the samples were stained with FITC-labeled goat anti-Rat IgG (Jackson ImmunoResearch, West Grove, PA). For intracellular staining, blood cells were fixed and permeabilized with Cytofix/Cytoperm (BD Biosciences) before staining. Fibrinogen binding was measured by staining the whole blood with PE-anti-mouse integrin αIIb mAb and FITC-anti-fibrinogen polyclonal antibody (pAb) (Emfret Analytics). For platelet activation analysis, whole blood was incubated with APC-labeled fibrinogen in the presence of 10 μg/ml of CRP. GPIbα shedding was evaluated using a DyLight 649-labeled mAb that specifically recognizes the N-terminal 45 kDa domain of mGPIbα (Xia.G5, Emfret Analytics). Platelets were gated by staining with DyLight488 labeled anti-mGPIbβ mAb (Emfret Analytics).

Confocal microscopy

Washed platelets from Abcg8$^{-/-}$ mice fed with low or high plant sterol diet were settled on slides by cytospin and fixed with 4% paraformaldehyde at 4°C for 30 minutes. The slides were

washed 3 times with PBS and then permeabilized by 0.2% Tx-100 in PBS for 15 min at room temperature. After two wash with PBS/2% FBS, platelets were incubated with rabbit anti-FlnA antibody and DyLight488 labeled anti-mGPIbβ mAb (Emfret Analytics) followed by incubation with AlexaFluor647-labeled goat anti-rabbit IgG. Fluorescent signals were detected using confocal microscope (Olympus FV1000-MPE Multiphoton Microscope, Olympus Corporation, Tokyo, Japan) and a UPlanSApo 100 x/1.4 Oil ∞ /0.17/FN26.5 objective (Olympus, Center Valley, PA).

Histopathology

Four Abcg8$^{-/-}$ female mice at 5 weeks of age were fed moderate plant sterol diets (high plant sterol diets for 6 weeks, low plant sterol diets for 5 weeks), or high plant sterol diets for 11 weeks. Heart, brain, spleen, kidney, liver, lung, femur were collected from mice after transcardial perfusion with phosphate-buffered saline (PBS) followed by immersion-fixation in formaldehyde; and were sent to the Histology Laboratory at Charles River Laboratories International, Inc. (Wilmington, MA) for pathologic analysis. Formalin-fixed tissues were embedded in paraffin, sectioned at 5 micrometers, followed by staining with hematoxylin and eosin (H&E) and visualized on an Olympus BH2 microscope with SPlan objectives. Images were captured using an Olympus DP70 digital color camera.

Plasma glycocalicin determination

Plasma glycocalicin levels in human plasma samples were measured by ELISA using mouse mAb 142.16 as the capture antibody and biotinylated 142.2 as the detection antibody. A standard curve was constructed using serial dilutions of SSC/ISTH Secondary Coagulation Standard Lot#3. Both 142.16 and 142.2 mAbs were generated in our laboratory.

Statistics

Data are presented as mean ± SD as indicated. Two groups were compared by the unpaired Student *t* test (Prism, GraphPad Software Inc, San Diego, CA, USA). Probability values less than 0.05 were considered statistically significant.

Reference List

1. Kanaji T, Ware J, Okamura T, Newman PJ. GPIbα regulates platelet size by controlling the subcellular localization of filamin. *Blood* 2012;119:2906-2913.

2. Kanaji T, Russell S, Cunningham J et al. Megakaryocyte proliferation and ploidy regulated by the cytoplasmic tail of glycoprotein Ibα. *Blood* 2004;104:3161-3168.

3. Dole VS, Matuskova J, Vasile E et al. Thrombocytopenia and platelet abnormalities in high-density lipoprotein receptor-deficient mice. *Arterioscler Thromb Vasc Biol* 2008;28:1111-1116.

Supplemental Figure 1 - Impaired response of Abcg8$^{-/-}$ HS platelets to stimulation by thrombin and calcium ionophore. Abcg8$^{-/-}$ LS and Abcg8$^{-/-}$ HS platelets were stimulated with thrombin (0.4 U/ml), and calcium ionophore (2 μM) in the presence of APC-labeled fibrinogen for 10 minutes at room temperature. Samples were fixed, permeabilized, and stained with anti-FlnA antibody and analyzed by flow cytometry as described in Figure 4.

Supplemental Figure 2 - Dose-dependent effects of plant sterol accumulation in Abcg8$^{-/-}$ mouse organs. Organs from Abcg8$^{-/-}$ mice loaded either with moderate plant sterol (MS; panels A, C, E, G, I) or high plant sterol (HS; panels B, D, F, H, J) were harvested for histologic analysis. (A, B) BM from both groups showed increased numbers of megakaryocytes (C, D) Spleens from Abcg8$^{-/-}$ MS mice showed extramedullary hematopoiesis (C) which was more prominent in Abcg8$^{-/-}$ HS (D). (E, F) Extramedullary hematopoiesis (black arrow) and hepatitis (green arrow) are observed in the livers of Abcg8$^{-/-}$ HS mice (F). (G, H) Extramedullary hematopoiesis and bone marrow emboli within pulmon-ary vessels is shown in the lung section of Abcg8$^{-/-}$ mice fed a HS diet (H). Lungs of mice fed MS diet had normal histology (G). (I, J) Myocardial degeneration and multifocal histiocytic infiltration is observed in Abcg8$^{-/-}$ mice fed a HS diet.

Supplemental Figure 3 - Mitochondrial membrane potential ($\Delta\Psi_m$) is not disrupted in sitosterolemic platelets**.** Mitochondrial membrane potential (ΔΨm) was measured using MitoTracker Red CMXRos as an indicator dye in the presence or absence of carbonyl cyanide m-chlorophenylhydrazone (CCCP), a lipid-soluble amphipathic molecule that uncouples

oxidative phosphorylation.[46] Note that the degree of MitoTracker staining correlated well with platelet size, but was not disproportionally altered in platelets from Abcg8$^{-/-}$ HS versus GPIb-deficient platelets.

Supplemental Figure 4 - Proposed mechanism for the paradoxical phenotype of bleeding and atherosclerosis in sitosterolemia. Accumulation of phytosterols in red cell membranes results in hemolysis and anemia. Partitioning of plant sterols in the vessel wall undoubtedly contributes to the increased risk of atherosclerosis seen in sitosterolemic patients. Intercalation of plant sterols into megakaryocyte and platelet membranes has multiple disruptive effects – mostly activating in nature. Accumulated phytosterols also likely induce integrin clustering, leading to fibrinogen binding and internalization of integrin αIIbβ. Calcium flux accompanying this event leads to activation of platelet calpain, which cleaves filamin – a key intracellular adaptor protein that stabilizes plasma membrane/membrane skeleton interactions during platelet biogenesis. Filamin also controls trafficking of GPIbα to the plasma membrane, and positions the tyrosine kinase Syk – a key component in platelet activation downstream of collagen binding – near the ITAM tyrosines of the GPVI/FcRγ-chain complex. Disturbing the cellular locations of these key regulatory components combines to yield platelets with impaired adhesion to VWF and collagen under condition of shear, likely explaining the bleeding diathesis seen in likely explaining the bleeding diathesis seen in sitosterolemic patients.

Figure S1

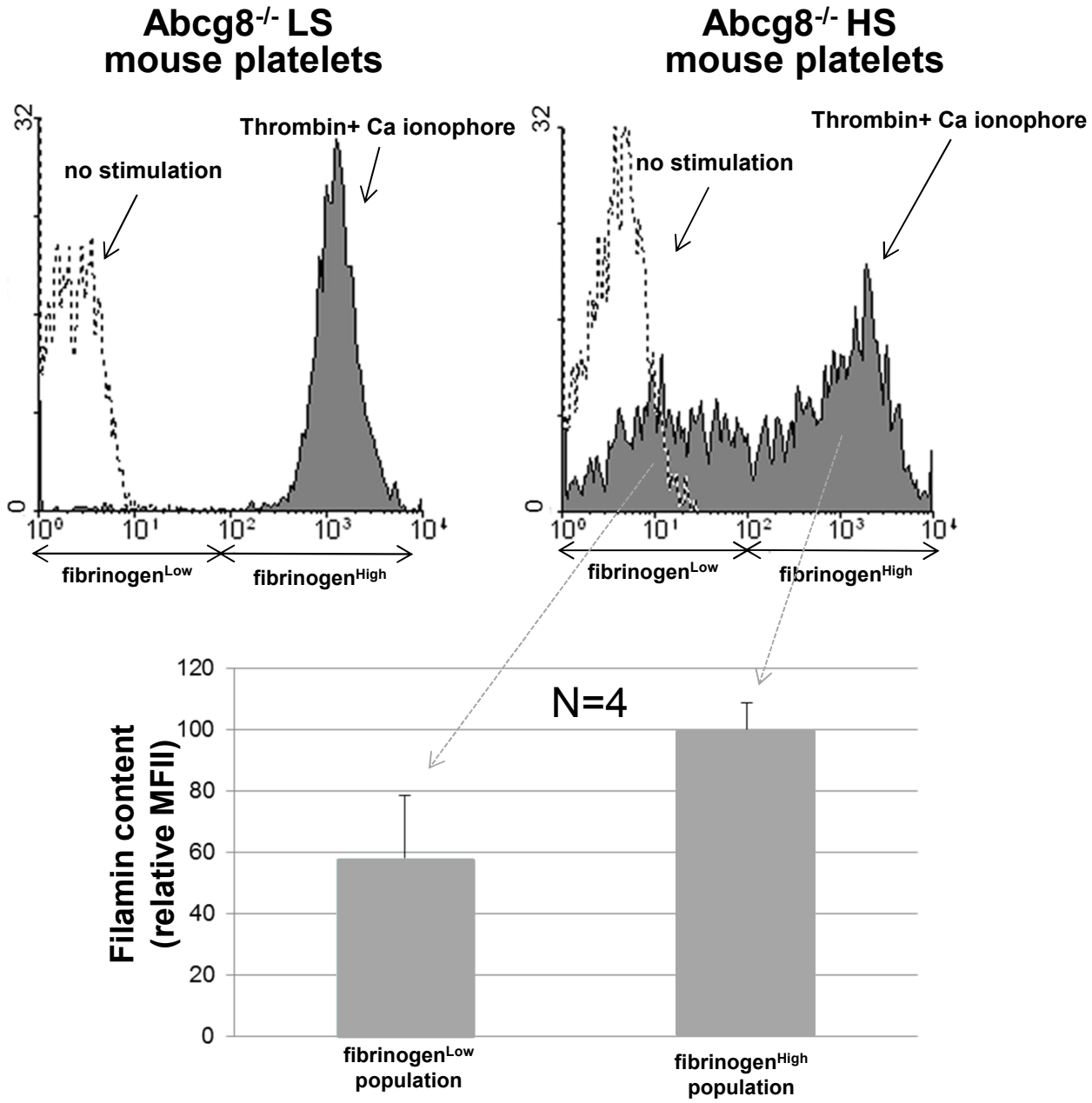
Abcg8-/- LS mouse platelets
Abcg8-/- HS mouse platelets
Thrombin+ Ca ionophore
no stimulation
32
0
10⁰
10¹
10²
10³
10⁴
fibrinogenLow
fibrinogenHigh
N=4
Filamin content (relative MFI)
120
100
80
60
40
20
0
fibrinogenLow population
fibrinogenHigh population

Figure S2

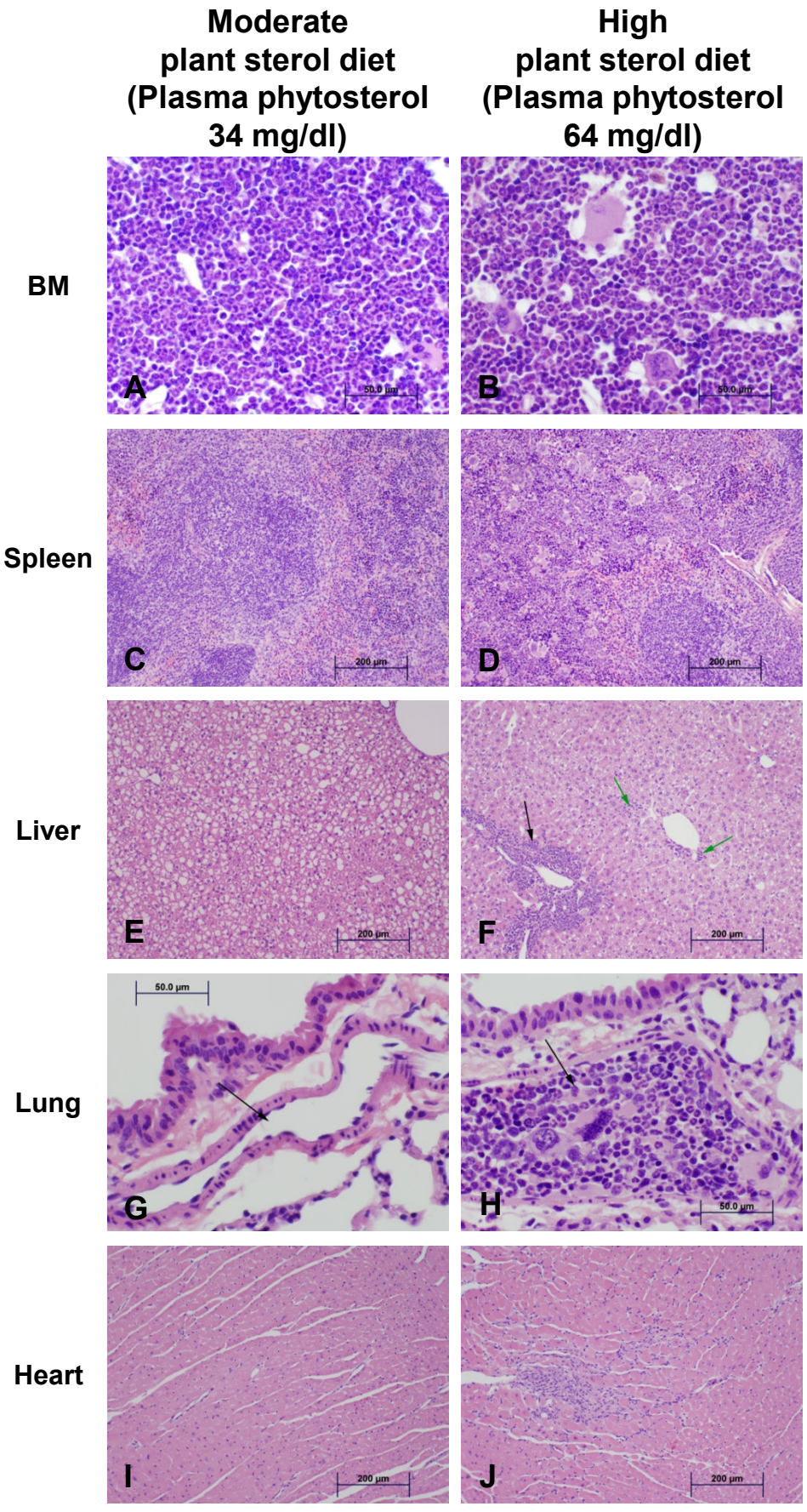
Moderate plant sterol diet (Plasma phytosterol 34 mg/dl)
High plant sterol diet (Plasma phytosterol 64 mg/dl)
BM
Spleen
Liver
Lung
Heart
A
B
C
D
E
F
G
H
I
J
50.0 µm
200 µm

Figure S3

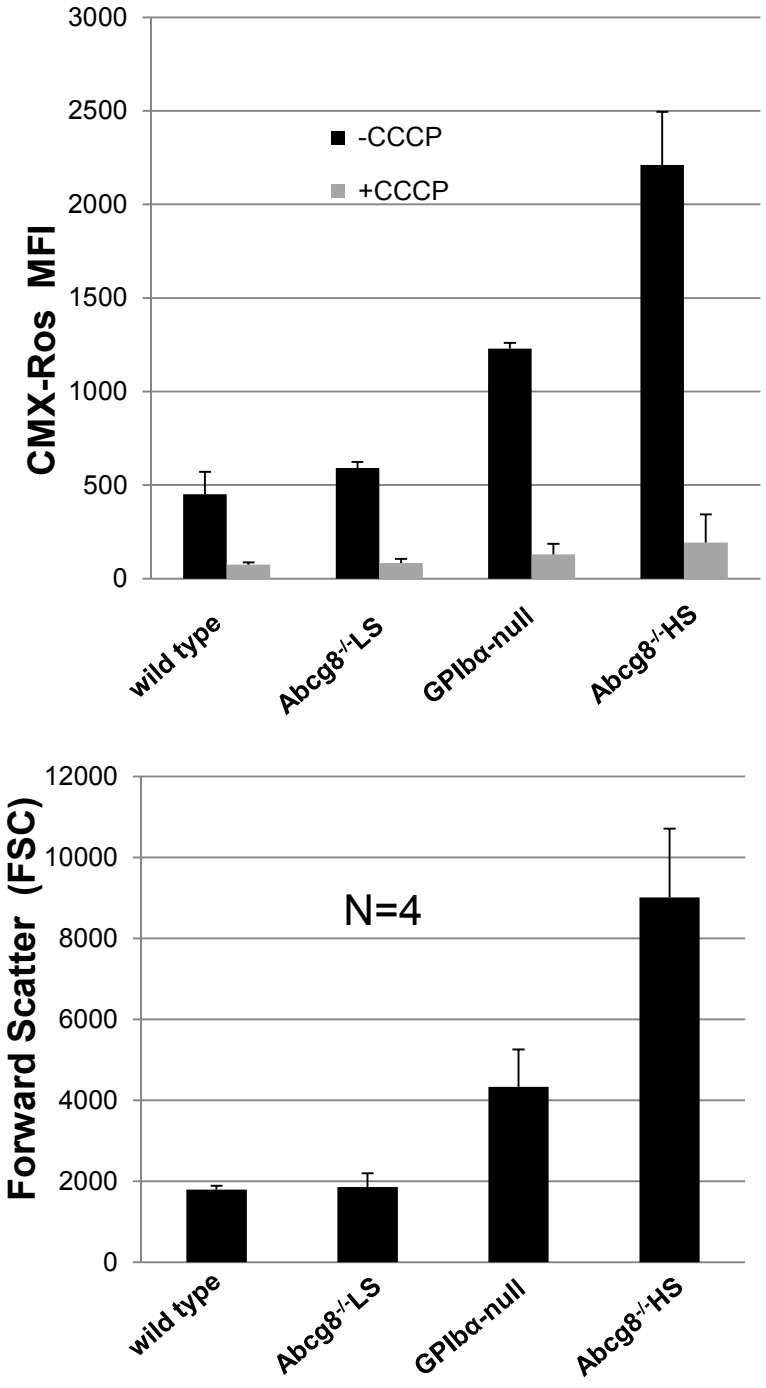

CCCP: carbonyl cyanide m-chlorophenylhydrazone - a lipid-soluble amphipathic molecule that uncouples oxidative phosphorylation

Figure S4

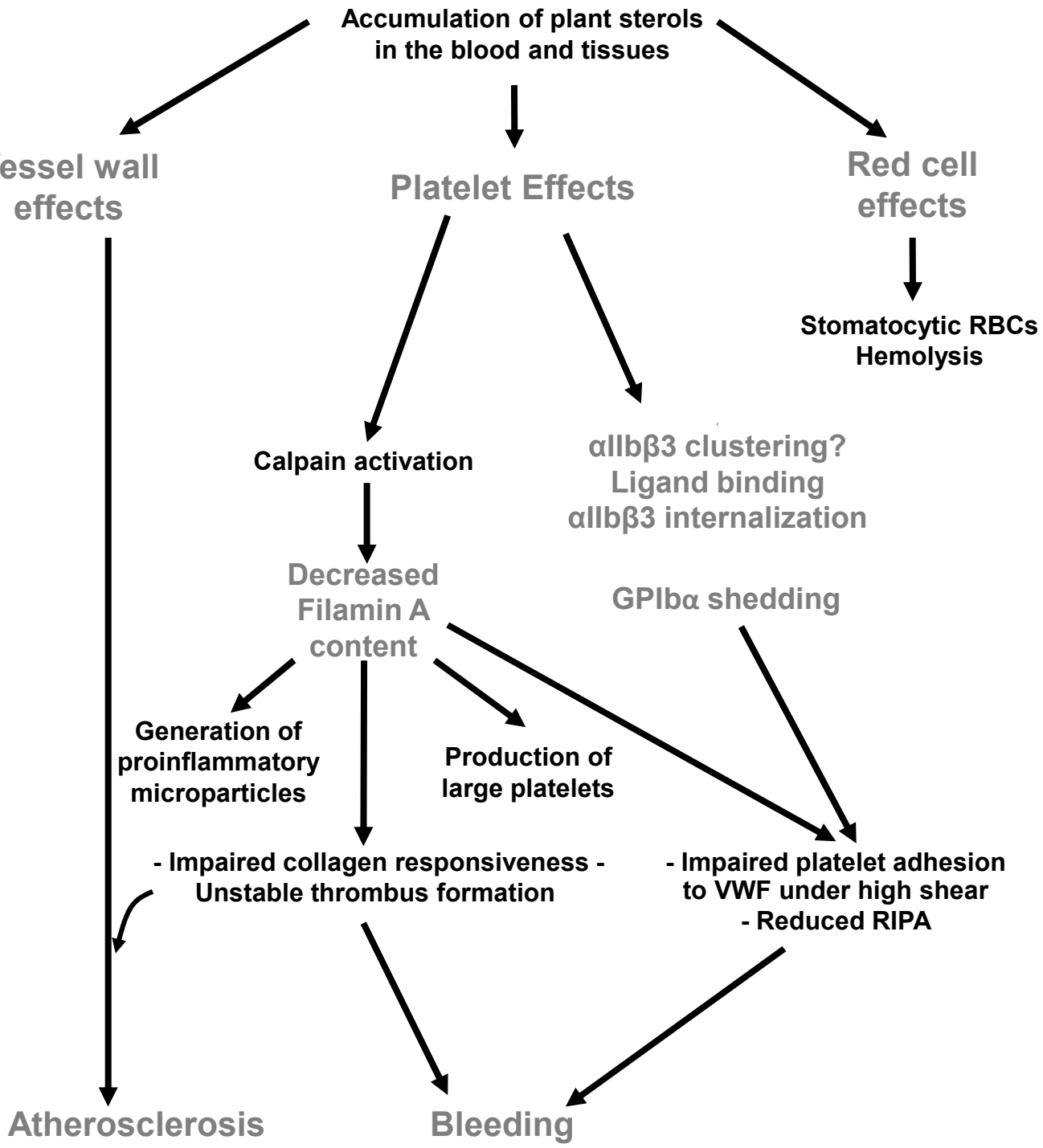
Accumulation of plant sterols in the blood and tissues
Vessel wall effects
Platelet Effects
Red cell effects
Stomatocytic RBCs Hemolysis
Calpain activation
αIIbβ3 clustering? Ligand binding αIIbβ3 internalization
Decreased Filamin A content
GPIbα shedding
Generation of proinflammatory microparticles
Production of large platelets
- Impaired collagen responsiveness - Unstable thrombus formation
- Impaired platelet adhesion to VWF under high shear - Reduced RIPA
Atherosclerosis
Bleeding